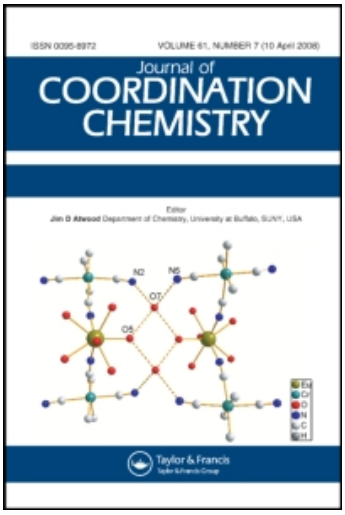

Journal of Coordination Chemistry
Publication details, including instructions for authors and subscription information:
http://www.informaworld.com/smpp/title~content=t713455674

Synthesis, crystal structure and characterization of a series of complexes constructed from coordinated Lanthanides(III) and the heteropolyanion $[SiMo_{12}O_{40}]^{4-}$

Qiu-Xia Han[a]; Jing-Ping Wang[b]; Jing-Yang Niu[b]
[a] Basic Experiment Teaching Center, Henan University, Institute of Molecular and Crystal Engineering, Kaifeng 475001, P.R. China [b] School of Chemistry and Chemical Engineerng, Henan University, Kaifeng 475001, P.R. China

To cite this Article Han, Qiu-Xia , Wang, Jing-Ping and Niu, Jing-Yang(2007) 'Synthesis, crystal structure and characterization of a series of complexes constructed from coordinated Lanthanides(III) and the heteropolyanion $[SiMo_{12}O_{40}]^{4-}$', Journal of Coordination Chemistry, 60: 12, 1303 — 1315
To link to this Article: DOI: 10.1080/00958970601062397
URL: http://dx.doi.org/10.1080/00958970601062397

Journal of Coordination Chemistry
Vol. 60, No. 12, 15 June 2007, 1303–1315

Synthesis, crystal structure and characterization of a series of complexes constructed from coordinated Lanthanides(III) and the heteropolyanion $[SiMo_{12}O_{40}]^{4-}$

QIU-XIA HAN†, JING-PING WANG‡ and JING-YANG NIU*‡

†Institute of Molecular and Crystal Engineering,
Basic Experiment Teaching Center, Henan University, Kaifeng 475001, P.R. China
‡School of Chemistry and Chemical Engineerng, Henan University,
Kaifeng 475001, P.R. China

(*Received 29 March 2006; in final form 30 March 2006*)

The reaction of α-$[SiMo_{12}O_{40}]^{4-}$ with trivalent cations Ln^{3+} and *N*-methyl-2-pyrrolidone leads to a series of complexes of formula $[Ln(NMP)_4(H_2O)_n]H[SiMo_{12}O_{40}]\cdot 2NMP\cdot mH_2O$ [where Ln = La (**1**), Pr (**2**), Nd (**3**), Sm (**4**), Gd (**5**), $n = 4$, Ln = Dy (**6**), Er (**7**), $n = 3$. NMP = *N*-methyl-2-pyrrolidone]. The syntheses, X-ray crystal structures, IR, and ESR spectra and thermal properties of the complexes **1**, **2**, **4**, **6**, **7** have been reported previously. Here, we report X-ray crystal structures, IR, UV, ESR spectra and thermal properties of the complexes $[Nd(NMP)_4(H_2O)_4]H[SiMo_{12}O_{40}]\cdot 2NMP\cdot 1.5H_2O$ **(3)**, and $[Gd(NMP)_4(H_2O)_4]H[SiMo_{12}O_{40}]\cdot 2NMP\cdot H_2O$ **(5)**. In addition, the electrochemical behaviour of this series of complexes in aqueous solution and aqueous-organic solution has been investigated and systematic comparisons have been made. All these complexes exhibit successive reduction process of the Mo atoms.

Keywords: Crystal structure; Electrochemical; Lanthanide(III); Heteropolyanion

1. Introduction

Interest in the study of polyoxometalates (POMs) remains at a high level due to their wide range of properties in several fields [1–3]. In particular, the results from electrochemical investigations by this group and others, which establish the existence of catalytic properties for heteropolyanions have been reviewed recently [4]. New results concern the ability of one- and two-electron reduced heteropolyanions of the Keggin and Dawson series to convert quantitatively NO into N_2O in acidic aqueous media. α-$SiMo_{12}O_{40}^{4-}$ has been used as an electrocatalyst for chlorate ion reduced by the six-electron reduced species in the presence of protons to yield chloride and water and in the presence of chlorate ions in 50% (v/v) dioxane–water solution containing

*Corresponding author. Email: jyniu@henu.edu.cn

ISSN 0095-8972 print/ISSN 1029-0389 online © 2007 Taylor & Francis
DOI: 10.1080/00958970601062397

0.5 M H_2SO_4 [5]. Such achievements have stimulated our interest in the synthesis of this series of Keggin polyoxoanion with metal–organic complex moieties, with the aim of investigating their electrocatalytic behaviours.

Lanthanide ions have large radii and higher coordination numbers than transition metals, as well as luminescent properties for fluorescent probes, and so their introduction into metal–organic frameworks may generate polymers with distinctive molecular structures and unusual properties. A series of complexes combining rare earth metals with unsaturated heteropolyanions have been isolated [6–9]. However, structures composed of rare earth elements and saturated heteropolyanions, such as α-$[SiMo_{12}O_{40}]^{4-}$ are still rare. In many cases, oxygen atoms on the surface of POMs are rather reactive and easily combine with the highly oxophilic rare earth ions to form precipitates instead of crystallization. We recently chose *N*-methyl-2-pyrrolidone as a protecting ligand and isolated single crystals of this series of lanthanide-containing polyoxometalate complexes.

The aim of the present article is to investigate the crystal structures, physical characterizations and thermal properties of this series of complexes. We also present a systematic study of the electrochemical behaviour by cyclic voltammetry (CV), as well as a study of their ESR spectra.

2. Experimental

2.1. *General*

2.1.1. Materials. $NdCl_3 \cdot 8H_2O$ and $GdCl_3 \cdot 6H_2O$ were prepared by dissolving their respective oxides in hydrochloric acid followed by drying. All organic solvents used for synthesis and physical measurements were reagent grade and used without further purification. $H_4SiMo_{12}O_{40} \cdot nH_2O$ was prepared by the literature method and confirmed by IR and UV spectra [10].

2.1.2. Instrumentation. C, H and N elemental analyses were performed on a Perkin-Elmer 240C elemental analyser. IR spectra of samples were recorded in KBr pellets with a Nicolet 170 SXFT-IR spectrometer in the range of 4000–500 cm^{-1}. The UV spectra were observed in acetonitrile–water (v : v = 2 : 1) solution with an England Heλiosα spectrometer. Thermogravimetric analyses (TG-DTA) were performed in air on a Perkin Elmer-7 instrument. The ESR spectra of powders of the title complexes after becoming dark blue due to sunshine were recorded on a Bruker ER-200-D-SRC spectrometer at X-band at 110 K. Cyclic voltammetric measurements were performed on a LK98 microcomputer-based electrochemical system (LANLIKE, Tianjin).

2.2. *Syntheses*

$[Nd(NMP)_4(H_2O)_4][HSiMo_{12}O_{40}] \cdot 2NMP \cdot 1.5H_2O$ (3), $[Gd(NMP)_4(H_2O)_4][HSiMo_{12}O_{40}] \cdot 2NMP \cdot H_2O$ (5). The preparation procedure was similar to that already described [11]. Elemental analysis data: Anal. Calcd for **3** (%): C, 13.50; H, 2.48; N, 3.16.

Found: C, 13.46; H, 2.42; N, 3.08. Anal. Calcd for **5** (%): C, 13.53; H, 2.46; N, 3.16. Found: C, 13.48; H, 2.44; N, 3.08. IR spectrum (cm^{-1}) 1638(s), 1512(m), 1117(w), 900(m), 952(s), 863(m), 792(s) for **3**; 1638(s), 1513(m), 1116(w), 901(m), 952(m), 862(m), 790 for **5**.

2.3. *X-ray crystallographic study*

The crystal structures of **3** and **5** were determined from single crystal X-ray diffraction data. The intensity data were collected by Oscillation frame scans on a Rigaku RAXIS-IV image plate area detector with Mo-Kα ($\lambda = 0.71073$ Å) at 293 K. The crystal parameters and details of the structure solution and refinement are summarized in table 1. The structures were solved by direct methods and refined using full-matrix least-squares on F^2 using the SHELXTL 97 program [12]. Thermal vibrations were treated anisotropically for all non-hydrogen atoms. The hydrogen atoms were geometrically fixed to allow riding on the parent atoms to which they are attached. CCDC reference numbers 298877(3) and 195688(5).

3. Results and discussion

3.1. *Structure of complex 5*

X-ray analyses show that both the complexes are isostructural. The structures of the two complexes are shown in figures 1 and 2. As an example, compound **5** is described here, which consists of one discrete organic-group coordinated Gd(III) cation and one α-Keggin heteropolyanion, $SiMo_{12}O_{40}^{4-}$. They are combined by static electric force, and several free water and NMP molecules are also present in complexes, which do not directly interact with the metal ions but remain outside the coordination sphere.

Table 1. Summary of crystal data and refinement results for complexes **3** and **5**.

Complex	**3**	**5**
Formula	$C_{30}H_{66}Mo_{12}N_6O_{51.5}SiNd$	$C_{30}H_{65}Mo_{12}N_6O_{51}SiGd$
Molecular weight	2640.92	2662.50
Space group	$P2_1/c$	$P2_1/c$
Unit cell dimensions (Å, °)		
a	17.422(4)	17.429(4)
b	18.281(4)	18.315(4)
c	23.220(5)	23.217(5)
β	106.91(3)	106.77(3)
Z	4	4
Volume ($Å^3$)	7075(2)	7096(2)
Density ($g\,cm^{-3}$)	2.479	2.492
$F(000)$	5058	5108
θ range	1.65–25.00	1.65–25.00
Range of h, k, l	−20/20, −21/21, −27/26	−20/20, −21/21, −27/27
Reflection collected	19,837	20,771
Independent reflections	11,162	11,783
Final R indices	$R = 0.0358$	$R = 0.0406$
$[I > 2\sigma(I)]$	$wR = 0.0911$	$wR = 0.0928$
Largest different peak and hole ($e\,Å^{-3}$)	2.840, −0.884	1.591, −0.953

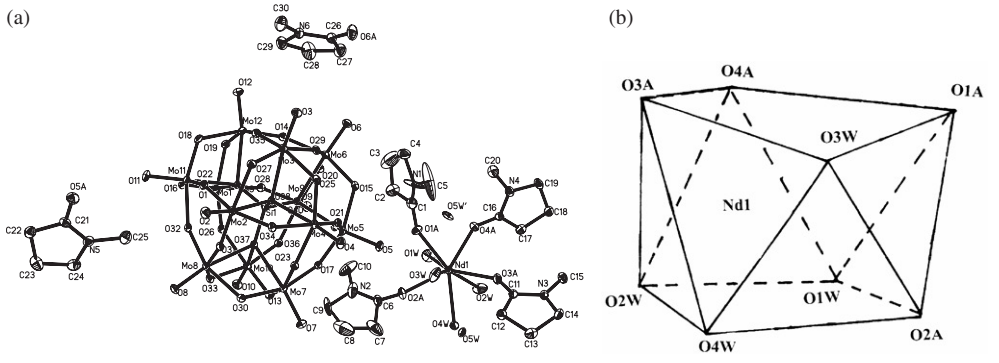

Figure 1. (a) Crystal structure of **3**; (b) Coordination polyhedron of Nd^{3+}.

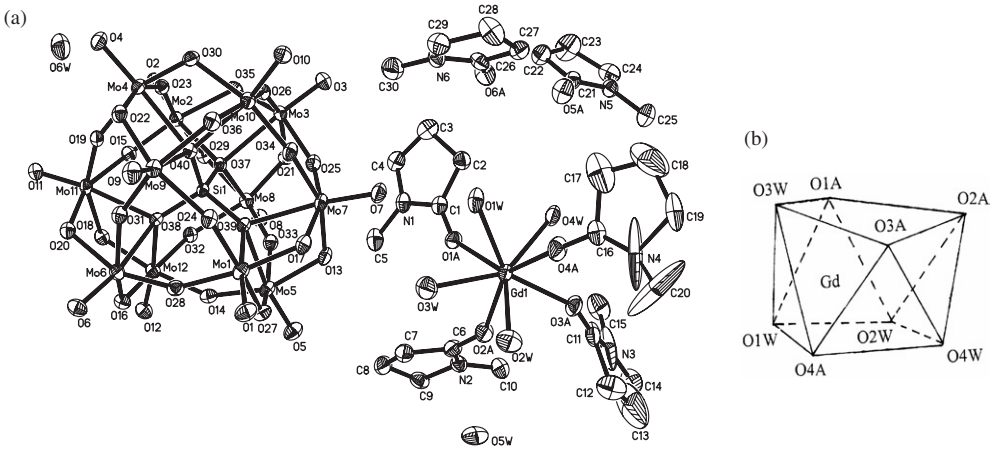

Figure 2. (a) Crystal structures of **5**; (b) Coordination polyhedron of Gd^{3+}.

The polyoxoanion of **5** exhibits a classical α-Keggin-type structure. Selected bond distances and angles relevant to the SiO_4 and MoO_6 groups are listed in table 2. The Si–O bond distances and O–Si–O angles of the four complexes are similar, ranging from 1.624(4)–1.638(4) Å, average 1.634 Å, and the O–Si–O mean bond angles are about 109.5° for **5**, within the cage, in good agreement with previously reported values [13].

For the MoO_6 octahedra, Mo–O_t distances range from 1.667(5)–1.707(5) Å, average 1.689 Å; Mo–O_a distances vary between 2.337(4)–2.372(4) Å, average 2.351 Å; Mo$-O_{b,c}$ distances varied between 1.810(7)–2.480(8) Å, average 1.932 Å. The coordination polyhedron of Gd^{3+} (figure 2b), shows O1A, O2A, O3A and O3W forming one basal plane of the square anti-prism while the other four oxygen atoms O1W, O2W, O4W and O4A form another basal plane; their average deviations are 0.0738 and 0.0220 Å, respectively. The Gd–O bond distances range from 2.312(6) to 2.480(6) Å, averaging 2.393 Å. Comparing the bond lengths of Gd–$O_{(NMP)}$ (average 2.336 Å) with those of Gd$-O_{(H_2O)}$ (average 2.450 Å), the former is 0.114 Å shorter.

Lanthanide contraction clearly affects the formation and crystal structure of the series of complexes. First, the coordination number decrease from **8** (La, Pr, Nd, Sm,

Table 2. Selected bond lengths (Å) and angles (°) of the polyanion for complexes **3** and **5**.

Si(1)–O(38)	1.626(4)	Si(1)–O(39)	1.627(4)
Si(1)–O(40)	1.628(4)	Si(1)–O(37)	1.635(4)
Mo(1)–O(1)	1.671(5)	Mo(1)–O(26)	1.826(4)
Mo(1)–O(16)	1.850(5)	Mo(1)–O(28)	2.013(5)
Mo(1)–O(19)	2.023(4)	Mo(1)–O(39)	2.371(4)
Mo(2)–O(2)	1.686(5)	Mo(2)–O(31)	1.814(4)
Mo(2)–O(34)	1.834(4)	Mo(2)–O(22)	2.020(5)
Mo(2)–O(27)	2.036(4)	Mo(2)–O(38)	2.362(4)
Mo(3)–O(3)	1.699(4)	Mo(3)–O(27)	1.822(4)
Mo(3)–O(35)	1.832(5)	Mo(3)–O(25)	2.014(4)
Mo(3)–O(29)	2.027(4)	Mo(3)–O(38)	2.344(4)
O(38)–Si(1)–O(39)	109.1(2)	O(38)–Si(1)–O(40)	109.1(2)
O(39)–Si(1)–O(40)	109.8(2)	O(38)–Si(1)–O(37)	110.0(2)
O(39)–Si(1)–O(37)	109.5(2)	O(40)–Si(1)–O(37)	109.3(2)
Nd(1)–O(2A)	2.359(5)	Nd(1)–O(4A)	2.375(5)
Nd(1)–O(1A)	2.387(5)	Nd(1)–O(3A)	2.399(5)
Nd(1)–O(1W)	2.477(6)	Nd(1)–O(2W)	2.524(6)
Nd(1)–O(4W)	2.527(5)	Nd(1)–O(3W)	2.534(5)
O(4A)–Nd(1)–O(1A)	75.0(2)	O(2A)–Nd(1)–O(4W)	68.74(19)
O(4A)–Nd(1)–O(3A)	77.91(19)	O(1A)–Nd(1)–O(3W)	67.91(19)
O(2A)–Nd(1)–O(1W)	76.6(2)	O(2W)–Nd(1)–O(4W)	71.07(18)
O(1W)–Nd(1)–O(2W)	69.5(2)	O(3A)–Nd(1)–O(3W)	77.87(18)
Si(1)–O(39)	1.624(4)	Si(1)–O(38)	1.635(4)
Si(1)–O(40)	1.638(4)	Si(1)–O(37)	1.638(4)
Mo(1)–O(1)	1.667(5)	Mo(1)–O(24)	1.830(5)
Mo(1)–O(17)	1.869(5)	Mo(1)–O(27)	2.026(5)
Mo(1)–O(28)	2.028(5)	Mo(1)–O(39)	2.372(4)
Mo(2)–O(2)	1.691(5)	Mo(2)–O(15)	1.823(5)
Mo(2)–O(29)	1.849(5)	Mo(2)–O(35)	2.033(5)
Mo(2)–O(23)	2.034(5)	Mo(2)–O(37)	2.337(4)
Mo(3)–O(3)	1.683(5)	Mo(3)–O(26)	1.814(5)
Mo(3)–O(35)	1.840(5)	Mo(3)–O(25)	2.025(5)
Mo(3)–O(21)	2.032(5)	Mo(3)–O(37)	2.359(4)
O(39)–Si(1)–O(38)	110.4(2)	O(39)–Si(1)–O(40)	109.6(2)
O(38)–Si(1)–O(40)	109.1(2)	O(39)–Si(1)–O(37)	109.1(2)
Gd(1)–O(4A)	2.312(6)	Gd(1)–O(2A)	2.317(5)
Gd(1)–O(3A)	2.349(6)	Gd(1)–O(1A)	2.366(5)
Gd(1)–O(4W)	2.395(7)	Gd(1)–O(2W)	2.461(7)
Gd(1)–O(3W)	2.464(6)	Gd(1)–O(1W)	2.480(6)
O(2A)–Gd(1)–O(3A)	74.5(2)	O(4A)–Gd(1)–O(4W)	76.3(3)
O(2A)–Gd(1)–O(1A)	77.1(2)	O(3A)–Gd(1)–O(1A)	121.5(2)
O(4A)–Gd(1)–O(2W)	109.1(3)	O(2W)–Gd(1)–O(1W)	70.3(2)
O(4W)–Gd(1)–O(2W)	70.3(3)	O(4A)–Gd(1)–O(1W)	69.0(2)
O(1A)–Gd(1)–O(3W)	77.8(2)	O(4W)–Gd(1)–O(1W)	113.5(2)

Gd) to **7** (Dy, Er) with decreasing ionic radius of the lanthanides; second, the Ln–O bond lengths decrease with increasing lanthanide atomic number (except for La): The mean Ln–O(NMP) (Å) distance follows in the order La–O(2.290) < Pr–O(2.396) > Nd–O(2.380) > Sm–O(2.349) > Gd-O(2.336) > Dy−O(2.282) > Er−O(2.224); the mean La–O(water) (Å) distance are 2.427, 2.518, 2.516, 2.495, 2.450, 2.293, 2.248 for La, Pr, Nd, Sm, Gd, Dy, Er, respectively. The Ln−O average bond distances (Å) of these complexes decreases in the series $La^{3+} < Pr^{3+} > Nd^{3+} > Sm^{3+} > Gd^{3+} > Dy^{3+} > Er^{3+}$, according to the increase in the ionic radii (Å): $La^{3+}(1.03) < Pr^{3+}(0.99) > Nd^{3+}(0.98) > Sm^{3+}(0.960) > Gd^{3+}(0.94) > Dy^{3+}(0.91) > Er^{3+}(0.89)$ [14]. As shown in figure 3, the Ln–O distances, from Pr to Er, present a decreasing tendency,

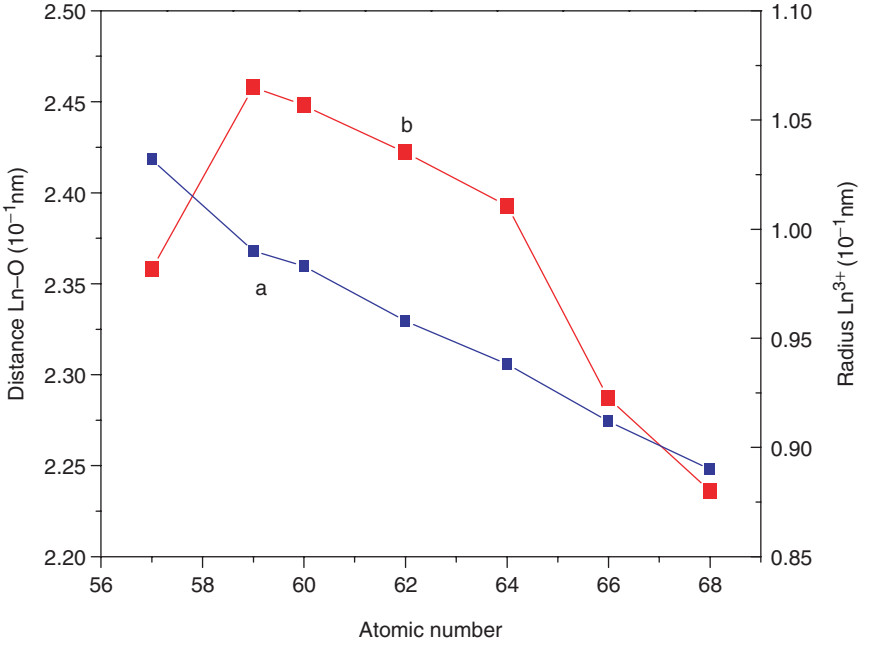

Figure 3. (a) Changes of ions radii with atomic number. (b) Changes of Ln–O distance with atomic number.

but not completely smooth. In the curve of Ln^{3+} radius, the La–O distance is irregular with $4f^0$ electron configuration letting La^{3+} bind firmly with ligands and the mean coordination bond distance shorter. Third, the considerable change in size of the Ln^{3+} ion means that homologous complexes of lanthanides with appreciably different radii may differ in structure. For example, $[Ln(NMP)_4(H_2O)_3]^{3+}$ coordinated ions with Ln = Dy and Er have different structures: the Dy has a distorted pentagonal bipyramid structure while the Er has a capped trigonal prism.

3.2. *Thermo-gravimetric studies*

The TG analyses of this series of complexes showed characteristic endothermal peaks in the range of 90–120°C, and two exothermal peaks in the region of 270–290°C and 460–490°C. The strong exothermic peak above 460–490°C is due to Ln−O bond breakage with oxidation of the organic fragment and the heteropoly anionic cage begining to decompose to lower oxides of the metals like MoO_3, and their slow volatilization [15].

Compound **5** will be our example. Thermal decomposition of **5** takes place in three main stages (shown in figure 4): the first step, below 115°C, leads to the loss of one free NMP and one free water (weight loss ca 4.4%), and an endothermal peak at 96.6°C is observed in the DTA; the second step, in the 115–375°C range, corresponds to the loss of four coordinated waters and one free NMP (weigh loss ca 6.43%); one exothermal peak at 282.5°C due to oxidation of NMP is observed; the last step, from 375–600°C to give a total of approximately 15.4% weight loss, corresponding to the loss of four coordinated NMP and half a constitution water (weigh loss ca 15.2%).

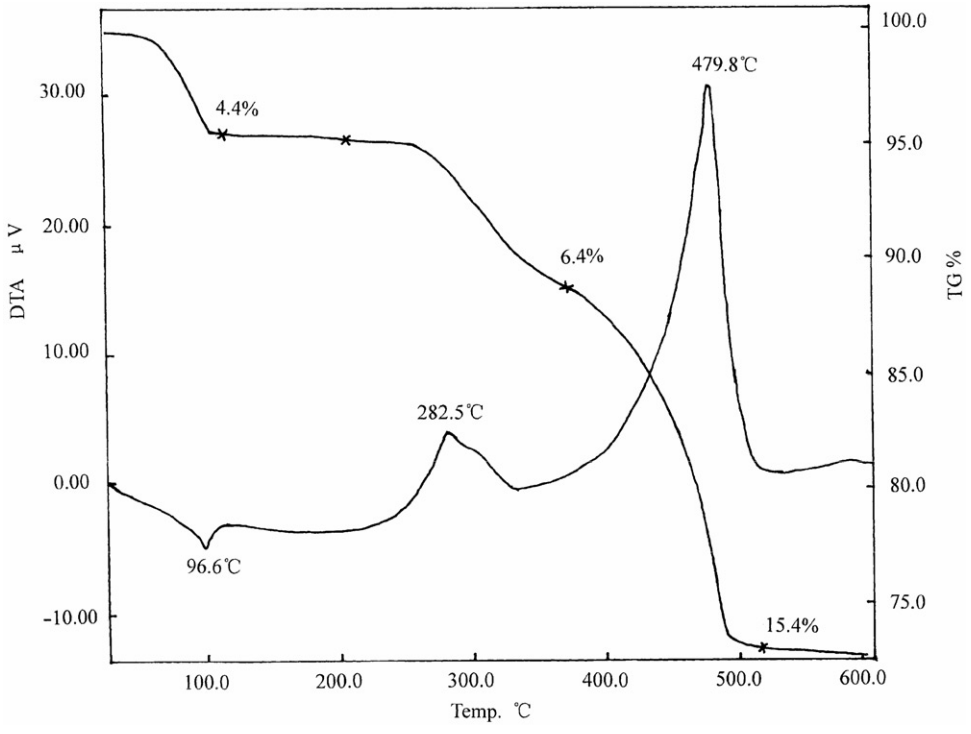

Figure 4. TG-DTA curves of **5**.

In the last step, one strong exothermal peak at 483°C is observed, due to oxidation of the organic fragment and indicates the Gd–O bonds break and the polyanion begins to decompose. Comparing the decomposition temperature with that of $H_4SiMo_{12}O_{40}$ [16], the result indicates the thermal stability of $SiMo_{12}O_{40}^{4-}$ in compound **5** is stronger than in the acid.

As shown in figure 5, slight changes in decomposition temperature of coordinated Ln(III) ions are found. The results indicate that the thermal stability is in the series La(483.3°C) > Pr(472°C) < Nd(473.2°C) < Sm(475.2°C) < Gd(483°C) = Dy(483.2°C) > Er(462°C), which is well compatible with that of the $Ln(OH)_3$: La(390°C) > Pr(328°C) < Nd(338°C) < Sm(345°C) < Gd(380°C) > Dy(300°C) > Er(255°C) (**14**). The most stable coordinated ions are La^{3+} and Gd^{3+} expected from the electronic configuration of Ln^{3+} and the extra stability associated with the formation of stable empty $4f^0$, half-filled $4f^7$ and filled $4f^{14}$ subshells. In addition, the temperatures for loss of coordinated water are lower than that for loss of NMP, further confirming stronger linkage between NMP and Ln^{3+} than between water and Ln^{3+}. The TG-DTA results are compatible with the X-ray structure analyses.

3.3. *ESR spectra*

Molybdenum is a favourable element for ESR spectroscopy. The intense photochromism exhibited by irradiating the pure solid sample in sunlight is assigned to the intervalence charge transfer ($Mo^{5+} \rightarrow Mo^{6+}$) IVCT band of $SiMo_{12}O_{40}^{4-}$, indicating that electron

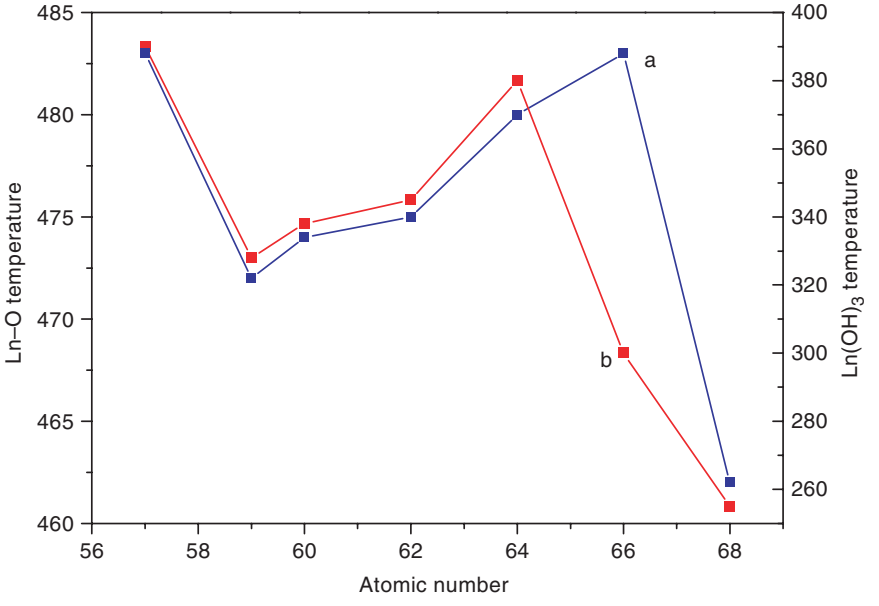

Figure 5. (a) Loss ligands temperature (°C) of coordination Ln^{3+}. (b) Loss water temperature (°C) of $Ln(OH)_3$.

transfer occurred between organic cation and inorganic anion, reducing $SiMo_{12}O_{40}^{4-}$ to heteropoly blue $SiMo_{12}O_{40}^{5-}$ with simultaneous oxidation of the organic cation [17–18].

Except for compound **5**, spectra for all compounds line in figure 6(a) show a shaped signal with the parameter g at about 1.944 [11]. In figure 6(a), we give the ESR line of complex **3**. Other signals could be observed in complex **5**, due to the special character of Gd^{3+}. As Gd^{3+} has an $^8S_{7/2}$ ground state, it is the only trivalent lanthanide whose ESR can be observed at room temperature. Since the spin–lattice relaxation time is shortened due to strong spin–orbit coupling in Gd^{3+} ions at low temperature, the ESR spectra of Gd^{3+} is more obvious at 110 K than at room temperature. As shown in figure 6(b), there are three groups of lines with effective g-values of approximately 5.98, 2.62 and 2.00, and wide absorption band for magnetic fields corresponding to $g<2$. Another g value of 1.938 is also found at 110 K.

3.4. *Electrochemistry*

The electrochemical behaviour of this series of complexes was mainly studied in aqueous media and aqueous–organic media by CV. All redox potentials ΔE_p(mV) and electron transfer number n, approximated by $E_{pa}(v)-E_{pc}(V)=57/n-63/n$ (mV) [19], for the reversible steps, are given in V *versus* SEC as obtained from CV ($\upsilon=20\,mV\,s^{-1}$) in 1 : 1 H_2SO_4 aqueous media. Cyclic voltammograms of the series of complexes show no remarkable differences compared with the α-$SiMo_{12}$ precursors in three subsequent steps in aqueous solutions 1 : 1 H_2SO_4 (figure 7a). From the CV data (table 3a), the first pair of peaks correspond to the $1e^-/1H^+$ redox process, while the other two pairs are undetermined according to the literature due to the possible

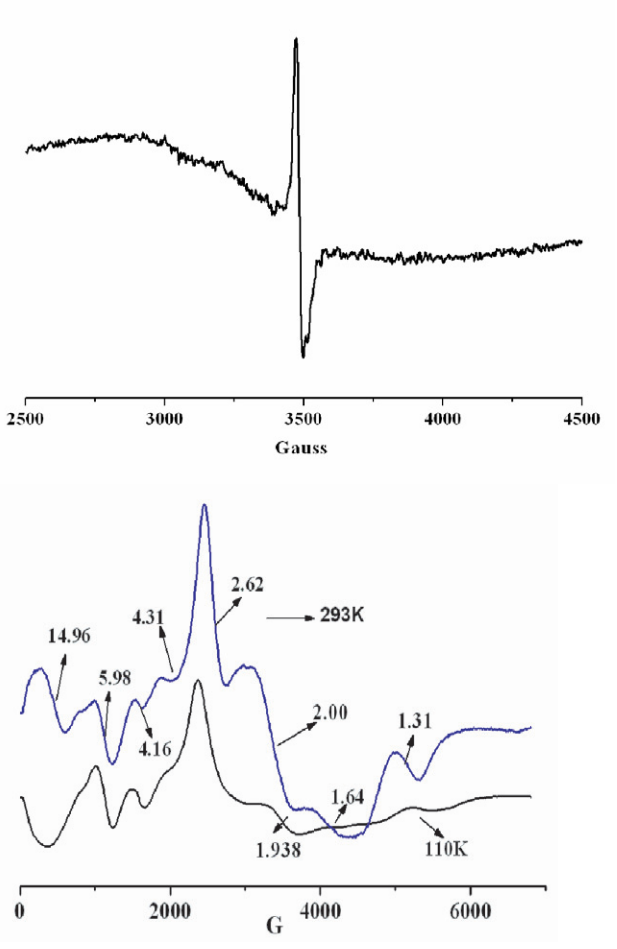

Figure 6. ESR spectra of the complexes **3** and **5** at 110 K.

occurrence of irreversible or quasi-reversible processes [20, 21]. The results indicate that although the lanthanide coordination cations are different, their influences on the polyanion are identical.

Therefore they are expected to generate a new series of heteropoly blues, giving rise to mixed-valence species in which delocalized electrons may coexist and interact with localized magnetic moments. For example, the CV of complex **5** shows three pairs of peaks with 1e, 2e, 2e redox processes, while the heteropoly blue consists of three pairs of peaks corresponding to the $1e^-/1H^+$ redox process, (see figure 7b).

Different media give different results. The change from one electron reduction to two-electron reduction on changing the medium from 1 : 1 H_2SO_4 to 1 M H_2SO_4 may be due to the different pH. This series of complexes are stable in the pH range 1–3 in both aqueous–organic media (figure 8a) and aqueous media (figure 8b). As an example, $[Gd(NMP)_4(H_2O)_4]H[SiMo_{12}O_{40}] \cdot 2NMP \cdot H_2O$ in aqueous–organic media shows an ill-defined cyclic voltammogram when $pH > 4$ and the peak current is much smaller; such an observation has previously been reported by Dong *et al.* in relation to Keggin-type polyoxometallates [22]. From the CV data in table 3(b) and the curves in

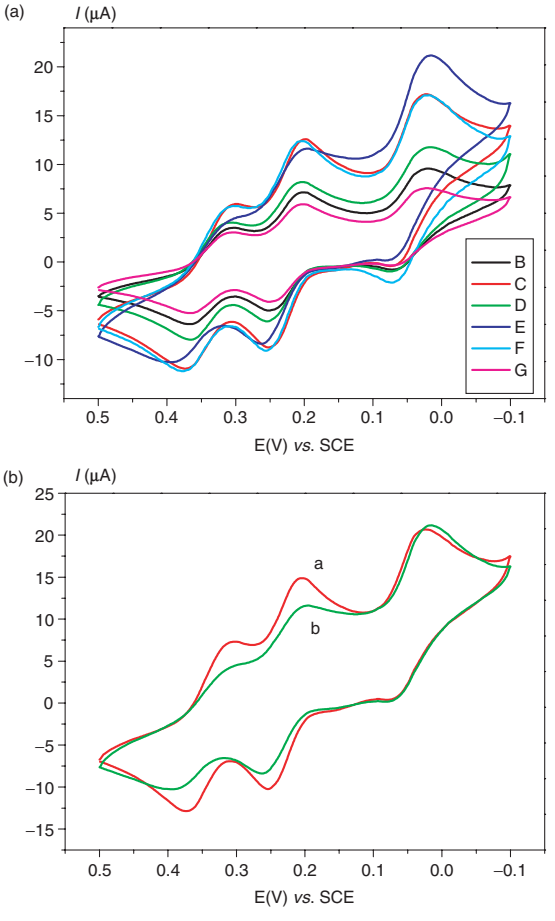

Figure 7. Cyclic voltammograms of all the series of complexes. (Conditions: glassy carbon working electrode, platinum counter electrode, SCE reference electrode, scan rate 20 m Vs^{-1}.) (a) CV of 1–7. B-La, C-Pr, D-Nd, E-Sm, F-Dy, G-Er. (b) CV of 5. a:before lighted b: heteropoly blue.

Table 3a. The CV data of complexes **1**–**7**.

	$1:1H_2SO_4$				$1:1H_2SO_4$		
Complex	E_{pa} (v)	E_{pc} (V)	ΔE_p (mV)	Complex	E_{pa} (v)	E_{pc} (V)	ΔE_p (mV)
1	0.3656	0.3010	62.5	**4**	0.3206	0.2706	50.0
	0.2512	0.2033	41.7		0.2029	0.1647	38.2
	0.0703	0.0205	49.8		0.0324	−0.0147	47.1
2	0.3749	0.2996	75.3	**6**	0.0367	0.3019	64.9
	0.2498	0.1988	51.0		0.2521	0.2023	49.8
	0.0726	0.0228	49.8		0.0714	0.0228	48.6
3	0.3656	0.3089	56.7	**7**	0.3761	0.3008	75.3
	0.2533	0.2030	50.3		0.2544	0.2023	52.1
	0.0726	0.0170	55.6		0.0703	0.0216	48.7
5	0.3726	0.3066	66.0	**5** heteropoly blue	0.3842	0.2961	88.1
	0.2544	0.2070	47.4		0.2625	0.1954	67.1
	0.0703	0.0274	42.9		0.0900	0.0170	73.0

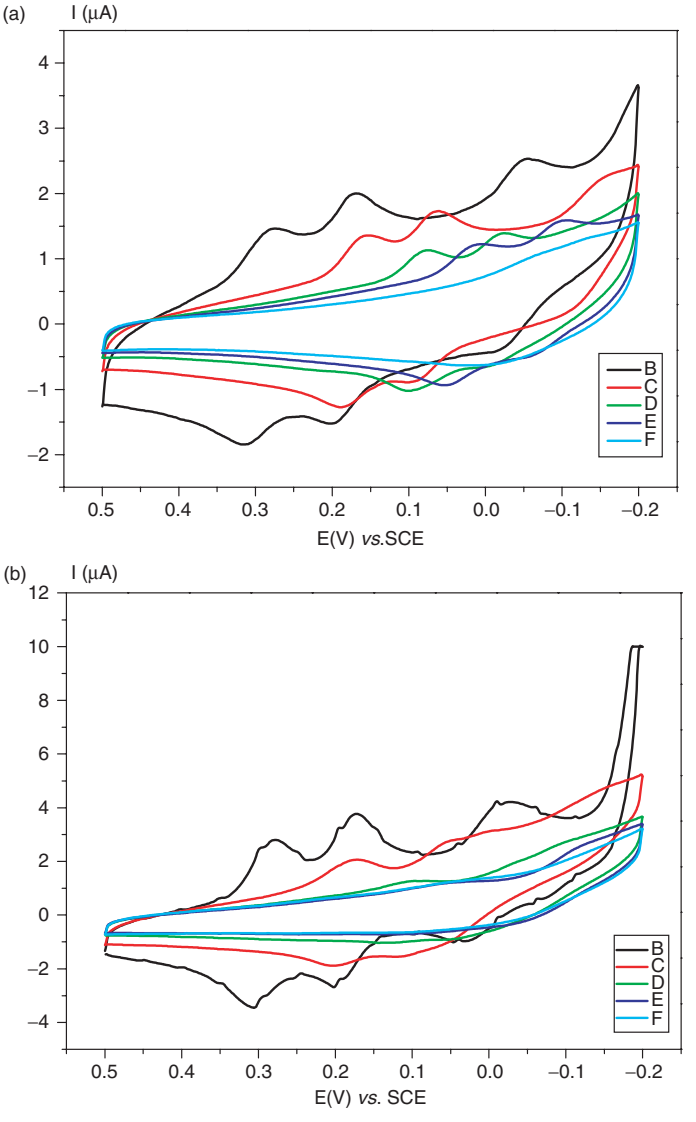

Figure 8. Cyclic voltammograms of $[Gd(NMP)_4(H_2O)_4]H[SiMo_{12}O_{40}]\cdot 2NMP\cdot H_2O$. Conditions: glassy carbon working electrode, platinum counter electrode, SCE reference electrode, scan rate $20\,m\,Vs^{-1}$, pH is adjusted by $0.5\,mol\,L^{-1}$ Na_2CO_3 solution. (a) In 1 M H_2SO_4 + 1,4-dioxane; v : v = 1 : 1; B: pH = 1, C: pH = 2, D: pH = 3, E: pH = 4, F: pH = 5; (b)1M H_2SO_4 B: pH = 1, C: pH = 2, D: pH = 3, E: pH = 4, F: pH = 5.

figure 8(a) and (b), we find the two-electron waves shifted to more negative potential and the current lower when the pH is increased; Launay *et al.* reported the pH effect of the first three reversible two-electron reductions [23]. In general the reduction of heteropolyanions is accompanied by protonation at low pH, and hence the pH of the solution has a great effect on the electrochemical behaviour of the compound. Cyclic voltammetry of aqueous–organic 1 mM $[Gd(NMP)_4(H_2O)_4]H[SiMo_{12}O_{40}]\cdot 2NMP\cdot H_2O$ solution [in $1\,mol\,L^{-1}$ H_2SO_4 + 1,4-dioxane (v : v = 1 : 1)

Table 3b. The CV data of complex **5**.

	1 : 1 (Organic-H_2SO_4)				($1\,mol\,L^{-1}H_2SO_4$)		
Compound	E_{pa} (v)	E_{pc} (V)	ΔE_p (mV)	Compound	E_{pa} (v)	E_{pc} (V)	ΔE_p (mV)
pH = 1	0.3162	0.2743	31.9	pH = 1	0.3081	0.2784	29.7
	0.2014	0.1689	32.5		0.2015	0.1737	27.6
	−0.0176	−0.0568	39.2		0.0324	−0.0009	33.3
pH = 2	0.1878	0.1527	35.1	pH = 2	0.2027	0.1716	31.1
	0.0946	0.0622	32.4		0.1081	0.0432	64.9
pH = 3	0.1014	0.0757	35.7	pH = 3	0.1311	0.0959	35.2
	−0.003	−0.0230	22.7				
pH = 4	0.0540	0.0054	48.6	pH = 4			
	−0.0514	−0.1054	54.0				

at pH = 1.00], consists of three pairs of peaks corresponding to the $2e^-/2H^+$ redox process. The reduction processes can be represented as follows [equations (1–3)].

$$SiMo_{12}O_{40}^{4-} + 2e + 2H^+ = H_2SiMo_{12}O_{40}^{4-} \quad (1)$$

$$H_2SiMo_{12}O_{40}^{4-} + 2e + 2H^+ = H_4SiMo_{12}O_{40}^{4-} \quad (2)$$

$$H_4SiMo_{12}O_{40}^{4-} + 2e + 2H^+ = H_6SiMo_{12}O_{40}^{4-} \quad (3)$$

Acknowledgement

This work was supported by Henan Innovation Project for University Prominent Research Talents and the Natural Science Foundation of Henan Province (No. 0524480020), and the Natural Science foundation of Henan University (XK04YBRW057).

References

[1] C.L. Hill. *Chem. Rev.*, **98**, 1 (1998).
[2] M.T. Pope. *Heteropoly and Isopoly Oxometalates*, Springer-Verlag, New York (1983).
[3] M.T. Pope, G.M. Varga. *Inorg. Chem.*, **5**, 1249 (1966).
[4] M. Sadajabe, E. Steckhan. *Chem. Rev.*, **98**, 219 (1998).
[5] K. Unoura, A. Iwashita, E. Itabashi, N. Tanaka. *Bull. Chem., Soc., Jpn.*, **57**, 597 (1984).
[6] X.D. Xi, G. Wang, B.F. Liu, S.J. Dong. *Electrochem. Acta*, **40**, 1025 (1995).
[7] M.T. Pope, M. Sadakane, M.H. Dickman. *Angew. Chem., Int. Ed.*, **39**, 2914 (2000).
[8] Q.H. Luo, R.C. Howell, M. Dankova, J. Bartis, *et al. Inorg. Chem.*, **40**, 1894 (2001).
[9] N. Haraguchi, Y. Okaue, T. Isobe, Y. Matsuda. *Inorg. Chem.*, **33**, 1015 (1994).
[10] C. Rocchiccioli-Deltcheff, M. Fournier, R. Franck, R. Thouvenot. *Inorg. Chem.*, **22**, 207 (1983).
[11] [Sm] J.P. Wang, Q.X. Han, J.Y. Niu. *Acta Chim. Sin.*, **8**, 1445 (2002); [La] J.P. Wang, Q.X. Han, J.Y. Niu. *J. Coord. Chem.*, **56**(11), 1003 (2003); [Dy] J.P. Wang, Q.X. Han, J.Y. Niu. *J. Coord. Chem.*, **57**(1), 33 (2004); [Pr] J.P. Wang, Q.X. Han, J.Y. Niu. *Trans. Met. Chem.*, **2**, 170 (2004); [Er] J.P. Wang, Q.X. Han, J.Y. Niu. *Chinese J. Struct. Chem.*, **23**(4), 425 **(**2004).
[12] G.M. Sheldrick. *SHELXTL 97*, *Programme for the Refinement of Crystal Structures*, University of Göttingen, Germany (1997).
[13] A.S.J. Wery, J.M. Gutierrez-Zorrilla, A. Luque, P. Vitoria, P. Roman, M. Martinez-Ripoll. *Polyhedron*, **17**, 1247 (1998).

[14] X.W. Yi, C.H. Huang, W. Wang, Y.J. Liu, J.G. Wu. *Inorganic Chemistry Books*, Vol. 7, p. 223, Science Press, Beijing (1998).
[15] R.C. Mackenjie. *Differential Thermal Analysis*, Acadimic, New York (1970).
[16] Z.P. Wang, J.Y. Niu, L. Xu. *Acta Chim. Sin*., **53**, 757 (1995).
[17] C. Sanchez, J. Livage, J.P. Launay, M. Fournier, Y. Jeannin. *J. Am. Chem. Soc*., **104**, 3194 (1982).
[18] J.N. Barrows, M.T. Pope. *Adv. Chem. Ser*., **226**, 403 (1990).
[19] H.B. Zhang, G.J. Wang, T.H. Wu. *Chem. J. Chinese Universities*, **5**, 656 (1991).
[20] N. Haraguchi, Y. Okaue, T. Isobe, Y. Matsuda. *Inorg. Chem*., **33**, 1015 (1994).
[21] S.G. Wang, J. Peng, M. Yu, Y.G. Chen, L.Y. Qu. *J. Chin. Inorg. Chem*., **9**, 364 (1993).
[22] L. Cheng, H. Seen, J. Liu, S. Dong. *J. Chem., Soc., Dalton Trans*., 2619 (1999).
[23] J.P. Launay, R. Massart, P.J. Souchary. *Less-CommonMet*., **36**, 139 (1974).